

Response of a laterally loaded pile group due to cyclic loading in clay

Jiangwei Shi^{1,2a}, Yuting Zhang^{3b}, Long Chen^{*1,2} and Zhongzhi Fu^{4c}

¹Key Laboratory of Ministry of Education for Geomechanics and Embankment Engineering, Hohai University, Nanjing 210024, China

²Jiangsu Research Center for Geotechnical Engineering Technology, Hohai University, Nanjing 210024, China

³Tianjin Research Institute for Water Transport Engineering, M.O.T., China

⁴Nanjing Hydraulic Research Institute, Geotechnical Engineering Department, Nanjing 210029, China

(Received August 1, 2017, Revised August 9, 2018, Accepted August 19, 2018)

Abstract. In offshore engineering, lateral cyclic loading may induce excessive lateral movement and bending strain in pile foundations. Previous studies mainly focused on deformation mechanisms of single piles due to lateral cyclic loading. In this paper, centrifuge model tests were conducted to investigate the response of a 2×2 pile group due to lateral cyclic loading in clay. After applying each loading-unloading cycle, the pile group cannot move back to its original location. It implies that residual movement and bending strain are induced in the pile group. This is because cyclic loading induces plastic deformation in the soil surrounding the piles. As the cyclic load increases from 62.5 to 375 kN, the ratio of the residual to the maximum pile head movements varies from 0.30 to 0.84. Moreover, the ratio of the residual to the maximum bending strains induced in the piles is in a range of 0.23 to 0.82. The bending strain induced in the front pile is up to 3.2 times as large as that in the rear pile. Thus, much more protection measures should be applied to the front piles to ensure the serviceability and safety of pile foundations.

Keywords: centrifuge modeling; cyclic loading; pile group; lateral movement; bending strain

1. Introduction

In marine deposits, pile foundations are commonly constructed to support various structures such as oil platforms. Lateral cyclic loading resulting from wave, wind and tide actions is inevitably applied to offshore structures. If excessive lateral movements and/or bending moments are induced in pile foundations, the serviceability and safety of offshore structures cannot be guaranteed. Thus, response of existing piles due to lateral cyclic loading has attracted increasing research attention (e.g., Long and Vanneste 1994, Rollins *et al.* 2006a, Achmus *et al.* 2009, Haldar and Babu 2010, Zhang and Ng 2017).

Field monitoring, centrifuge test and numerical analysis were conducted to investigate the performance of laterally loaded single piles due to cyclic loading in sands (e.g., Long and Vanneste 1994, Lin and Liao 1999, Brandenburg *et al.* 2005, Weaver *et al.* 2005, Rosquoet *et al.* 2007, Haldar and Babu 2010, Giannakos *et al.* 2012, Rahmani and Pak 2012) and clays (e.g., Zhang *et al.* 2011, Kuo *et al.* 2012, Kim and Jeong 2011, Memarpour *et al.* 2012, Wang *et al.* 2015). By conducting two-dimensional numerical parametric study, Haldar and Babu (2010) found that the

failure mechanisms of existing piles were significantly affected by the material and diameter of existing piles. Deformation mechanisms of pile-soil interaction were identified as soil densification and enlargement of resisting soil mass to a greater depth with cyclic loading (Giannakos *et al.* 2012).

However, much less attention was paid to the response of pile groups due to lateral cyclic loading (Rollins *et al.* 2005a, b, 2006a, b, Hussien *et al.* 2014). By conducting centrifuge tests in liquefiable sands, Rollins *et al.* (2005a, b) found that the lateral resistance of each pile was similar and about the same as that for the single pile. By conducting full-scale field tests and numerical analyses, Rollins *et al.* (2006a, b) found that group interaction effects decreased significantly as the pile spacing increased from 3.3 to 5.65 times of pile diameter.

Although a number of studies were conducted to explore response of existing piles due to lateral cyclic loading, previous studies mainly focused on deformation mechanisms of single piles. Investigation of pile group response due to cyclic loading in clay is relatively limited. In this study, centrifuge model tests were conducted to investigate the lateral movement, bending strain of a pile group due to lateral cyclic loading in clays.

2. Three-dimensional Centrifuge modelling

2.1 Experimental program and setup

Fig. 1 shows a plan view of the centrifuge model. The centrifuge tests were conducted at the Geotechnical Centrifuge Facility of the Hong Kong University of Science and Technology (Ng *et al.* 2001, 2002). The g- level (*N*)

*Corresponding author, Associate Professor
E-mail: longchenhhu@163.com

^aAssociate Professor
E-mail: ceshijiangwei@163.com

^bSenior Engineer
E-mail: tkszyt@163.com

^cSenior Engineer
E-mail: zzfu@nhri.cn

Table 1 Relevant scaling laws (Taylor 1995)

Parameter	Scaling law (model/prototype)
Gravity (m/s^2)	N
Length (m)	$1/N$
Strain	1
Stress (kPa)	1
Density (kg/m^3)	1
Unit weight (N/m^3)	N
Bending moment ($N\cdot m$)	$1/N^3$
Flexural stiffness ($N\cdot m^2$)	$1/N^4$
Time (consolidation / diffusion)	$1/N^2$

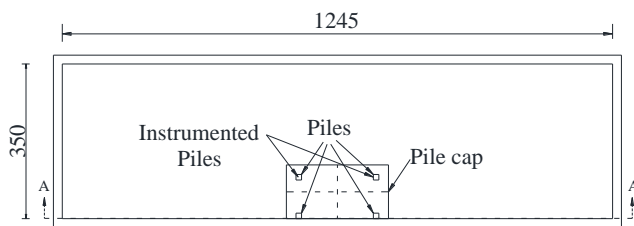


Fig. 1 Plan view of the centrifuge model (unit: mm)

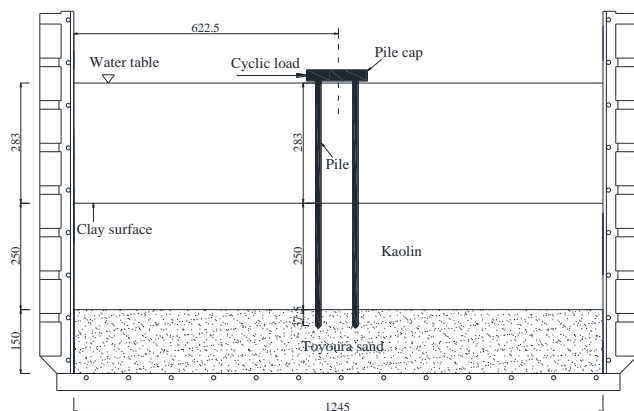


Fig. 2 Elevation view of the centrifuge model (unit: mm)

designed in this study was 40 g. The relevant scaling laws related to the centrifuge test were summarized in Table 1.

In this study, the length and width of the model container were 1245 mm (49.8 m in prototype) and 350 mm (14.0 m in prototype) in model scale, respectively. A 2×2 pile group was installed at the middle of the model container. The pile group was assumed to be wished-in-place. In other words, installation effects of the pile group was not simulated in the centrifuge test. Thus, the behavior of these four piles was closed to bored piles. The spacing of the pile group along the longitudinal and transverse directions of the model container was 175 mm and 87.5 mm, corresponding to 7 m and 3.5 m in prototype, respectively.

Fig. 2 shows an elevation view of the centrifuge model. A clay layer was located above a sandy layer. The thicknesses of the clay and sandy layers were 250 mm and 150 mm (i.e., corresponding to 10 m and 6 m in prototype), respectively. The pile group was penetrated into the sandy layer with a penetration depth of 37.5 mm, which was

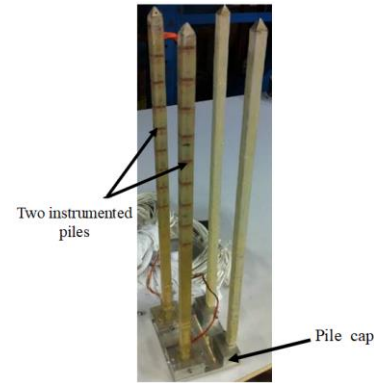


Fig. 3 Model pile group

equivalent to 1.5 m in prototype. In the centrifuge test, the ground water table was controlled at 283 mm above the clay surface, which was equivalent to 11.32 m in prototype. A hydraulic actuator was installed to apply lateral cyclic loading at the pile cap.

2.2 Model pile

Fig. 3 shows the model pile group used in the centrifuge test. It consisted of four rectangular hollow piles with a side length (L) of 12.7 mm (i.e., 0.508 m in prototype). Each model pile was made of an aluminum alloy tube with a Young's modulus (E_p) of 70 GPa. The model pile had a length of 22.8 m (i.e., 570.5 mm in model scale), a wall thickness of 63.2 mm (i.e., 1.58 mm in model scale) and flexural stiffness of $2.65 \times 10^2 \text{ MNm}^2$ in prototype. In literature, the moduli of elasticity of reinforced concrete were frequently reported in a range of 30 to 35 GPa (e.g., Lee and Ng, 2005; Liu *et al.*, 2009; Marshall, 2009). By taking the Young's modulus of concrete as 35 GPa, the model pile at 40 g was equivalent to a solid pile with a side length of 550 mm. In order to measure bending moments induced in the pile, semi-conductor strain gauges in terms of full Wheatstone bridge were installed along the piles. A protection layer made of epoxy with a thickness of 2 mm was applied to ensure the waterproof of strain gauges. The semi-conductor strain gauges used in this study had a gauge factor of 150, while the gauge factor of the conventional foil gauges was only 2. In other words, these semi-conductor strain gauges were much more sensitive than the conventional foil gauges. If variation of strain was larger than $1.5 \mu\epsilon$, it could be captured accurately by these semi-conductor strain gauges. In total, nine levels of strain gauges with a spacing of 35 mm (i.e., 1.4 m in prototype) were installed along the model pile. Based on the measured bending moments and the flexural stiffness of the model pile, bending strain of pile could be deduced.

2.3 Model preparation

Toyoura sand was adopted to prepare the sandy layer. In order to achieve a uniform sand sample, the pluvial deposition method was adopted in this study. The sand sample was prepared by raining sand from a hopper kept at a distance of 500 mm above the sand surface. Upon

Table 2 Summary of material properties of kaolin

Parameter	Value	Reference
Angle of internal shearing resistance at the critical state, ϕ' ($^{\circ}$)	22	Powrie (1986)
Specific volume of the critical state line at unit pressure, Γ	3.48	Phillips (1987)
Slope of one-dimensional compression line in $v \ln p'$ plane, λ	0.25	Al-Tabbaa (1987)
Slope of unload-reload line in $v \ln p'$ plane, κ	0.05	Al-Tabbaa (1987)
Coefficient of at-rest earth pressure, K_0	0.63	Jáky (1944)

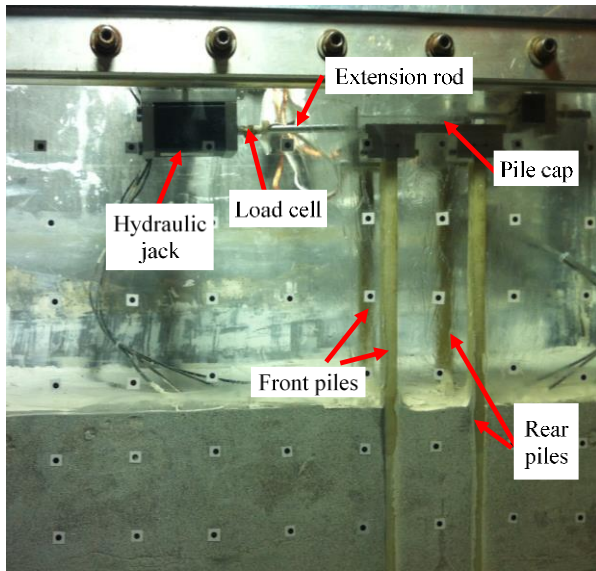


Fig. 4 A typical centrifuge model package

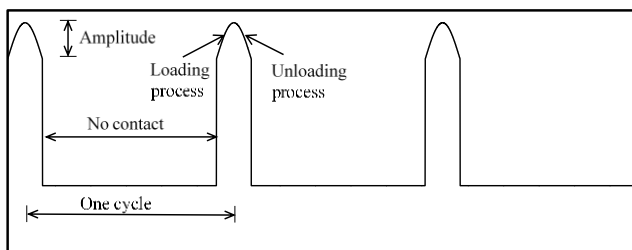


Fig. 5 Illustration of cyclic loading-unloading history

completion of sand preparation, the relative density of the sand layer was 70% (i.e., a medium sand sample). By connecting the sandy layer to a water tank, the sand was saturated.

The Speswhite kaolin powder was adopted to prepare the clay stratum. It had a liquid limit of 60% and angle of internal shearing resistance at the critical state of 22° (Powrie, 1986). Based on the empirical equation proposed by Jáky (1944), the coefficient of at-rest earth pressure was estimated as 0.63. Based on one-dimensional compression test, slopes of compression and unload-reload lines were 0.25 and 0.05, respectively (Al-Tabbaa 1987). A summary of material properties of kaolin was given in Table 2.

The Speswhite kaolin was mixed with a water content of 120 % under vacuum for 4 hours. In order to minimize the friction between the model container and the kaolin, silicon greases were applied on the inner surface of model

container. One dimensional consolidation was carried out after carefully pouring kaolin into the model container. At 1 g condition, five levels of vertical loadings were applied on the top of clay surface (i.e., 1, 5, 10, 20 and 30 kPa). Then, consolidation at 40 g was conducted by increasing the maximum vertical effective stress to 50 kPa at the clay surface. Using the empirical equation proposed by Asaoka (1978), the primary consolidation of clay was considered to be completed when the degree of consolidation reached 95%. Upon completion of the primary consolidation, the vertical surcharge load was removed. After completing the high-g consolidation, the saturated unit weight of clay was 16.8 kN/m^3 .

After clay preparation, the model pile group was installed at 1 g. Fig. 4 shows a typical centrifuge model package. Four holes with rectangular shape were drilled before the installation of the pile group. The loading system consisted of a hydraulic jack, an extension rod and a load cell. The hydraulic jack was fixed by an aluminum frame. The extension rod with a load cell was directly connected to the hydraulic jack. During the centrifuge test, variations of the applied lateral loads were measured by the load cell. A linear variable differential transformer (LVDT) was installed on the pile cap to measure the variation of the lateral movement of pile group. Before applying the lateral loads, about 1 mm gap was set between the extension rod and the pile raft. When the applied lateral load was increased, the extension rod moved forward to contact the pile cap, while the extension rod moved backward when the load was decreased.

2.4 Cyclic loading-unloading history

Fig. 5 illustrates the cyclic loading-unloading history applied on the pile group. Firstly, a loading signal was sent to the serve control system. Then, the extension rod moved forward to contact the pile cap gradually (i.e., loading process). After the extension rod reached the pile group, the applied load increased gradually until the load measured from the strain gauge was the same as the designed load. Then, the hydraulic jack gradually moved backward until the applied load became zero (i.e., unloading process). Finally, the extension rod kept moving backward until there was a gap between the extension rod and the pile cap (i.e., one loading-unloading cycle was completed). In this centrifuge test, the period of each loading-unloading cycle was designed as 54 seconds, which was equivalent to 1 day in prototype. The load condition adopted in this study was to simulate drag load from ships lied along wharf. According to the measurements in the Tianjin harbor, the lateral load applied on a single pile was typically ranged from 10 to 100 kN (Zhang and Ng 2017). For a two by two pile group, the applied load ranged from 62.5 to 375 kN.

2.5 Centrifuge testing procedures

After completing preparation of the centrifuge model (i.e., installation of pile group, loading system and transducers), the model container was transferred to the centrifuge arm. The ground water level was maintained by connecting the model container to a water tank. After the

reconsolidation of clay stratum at high g was reached, the lateral cyclic loading-unloading was applied. During the centrifuge tests, the pile head movement and bending strain of piles were measured simultaneously.

3. Interpretation of measured results

3.1 Variation of undrained shear strength with depth

Based on the method proposed by Asaoka (1978), the degree of consolidation of soil can be estimated. In-flight T-bar test is conducted when the degree of consolidation reaches 95%. Fig. 5 shows variation of the undrained shear strength of clay with depth. A constant T-bar factor of 10.5 is used to deduce the undrained shear strength (Randolph and Houlsby 1984). To gain a better understanding of the undrained shear strength, profiles of soil strength estimated from two empirical equations (i.e., Bolton and Stewart 1994, Gourvenec *et al.* 2009) are also included for comparison. Due to a smaller void ratio of soil at a deeper depth, both deduced and calculated undrained shear strengths of clay increase as an increase in the soil depth. The deduced undrained shear strength agrees well with the empirical equation proposed by Gourvenec *et al.* (2009), while it is much smaller than the predicted values given by the empirical equation of Bolton and Stewart (1994). This is because the empirical equations from Gourvenec *et al.* (2009) and Bolton and Stewart (1994) are proposed for undrained shear strengths in lightly and heavily overconsolidated clays, respectively. For the soil tested in this study, it is lightly overconsolidated soil.

3.2 Typical lateral pile head movements during cyclic loading

All the results presented are in prototype scale, unless stated otherwise. Fig. 7(a) shows typical lateral pile head movements due to cyclic loading. For these first two cycles, the applied maximum load and the load period are 62.5 kN and 1 day in prototype, respectively. During the loading process, the lateral movement induced in the pile head increases significantly, while it decreases dramatically when the applied is reduced. However, the pile head does not move back to its initial location. It is indicated that residual movements are induced in the pile group after each loading-unloading cycle. Note that this residual movement increases with the applied loading cycles. This is because accumulative plastic deformation is expected to be induced in the soil surrounding the existing piles during loading-unloading cycles.

Fig. 7(b) shows the variation of the lateral pile head movements with loading cycles. When the applied load is less than 125 kN, the maximum pile head movement is about 106 mm in prototype. By increasing the cyclic loading to 250 kN, the maximum pile head movement is as large as 1134 mm. It implies that significant plastic deformation is induced in the soil when the lateral load increases from 125 to 250 kN. As reported by Zhang *et al.* (2011), the stiffness of clay surrounding the existing piles decays as a result of lateral cyclic loadings. This can be proved by the picture shown in Fig.7(b). Cracks are induced

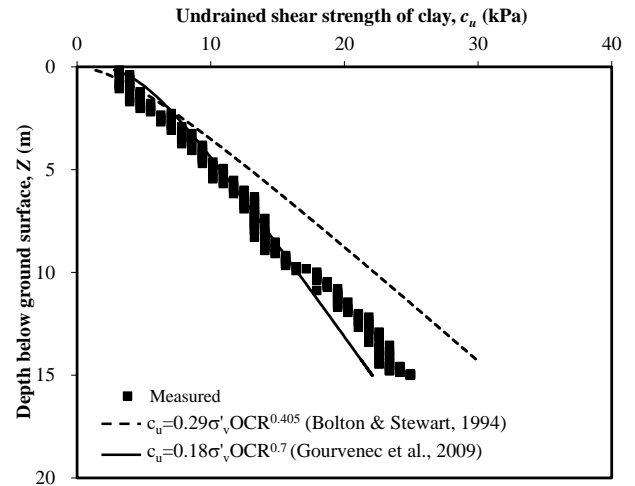
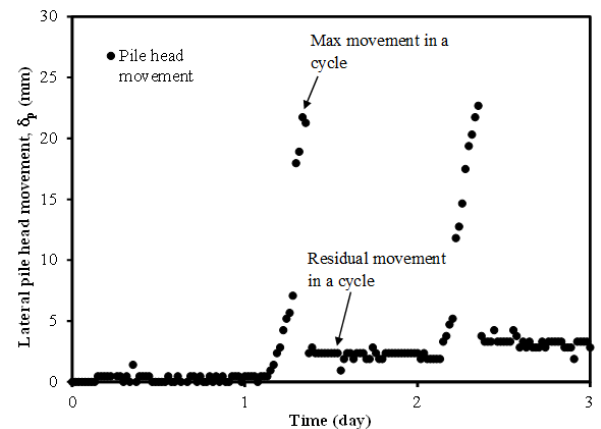
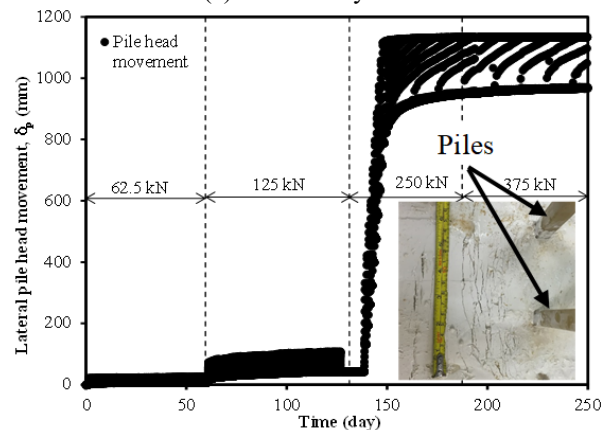


Fig. 6 Variation of the undrained shear strength of clay with depth



(a) First two cycles



(b) All cycles

Fig. 7 Typical lateral pile head movements during cyclic loading and unloading

in the soil surrounding the existing piles. Thus, the residual pile movement increases at an increased rate when the applied load is less than 250 kN. When the applied lateral load increases from 250 to 375 kN, a slight increase in the pile movement is observed. This may be due to the resisting soil mass gradually enlarges to a greater depth (Giannakos *et al.* 2012).

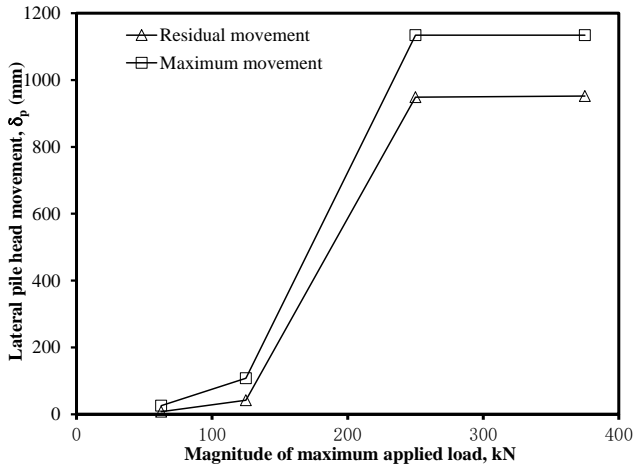


Fig. 8 Relationship between lateral pile head movement and applied cyclic load

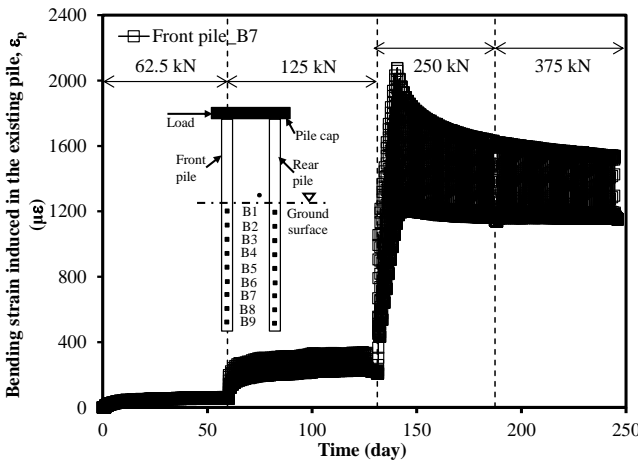


Fig. 9 Typical bending strain induced in the piles during cyclic loading and unloading

3.3 Relationship between lateral pile head movement and applied cyclic load

Fig. 8 shows the relationship between the lateral pile head movement and the applied load. When the applied load increases from 62.5 to 375 kN, the maximum and residual lateral movements induced in the pile cap varies from 26.0 to 1134 mm and 7.6 to 952 mm, respectively. When the applied load is equal to 250 kN, the resisting soil mass may reach the sandy layer which has much larger lateral resistance than clay layer. This may be the reason that the lateral movement at the pile cap increases slightly when the load increases from 250 to 375 kN.

As the maximum load increases from 62.5 to 375 kN, ratio of the residual pile head movement to the maximum pile head movement varies from 0.30 to 0.84. It means that large amount of the lateral pile head movement is recovered when the applied load is small (i.e., 62.5 and 125 kN). This is because a small load induces small plastic deformation in the soil surrounding the piles. However, only 16% of the maximum pile head movement is recovered when the applied maximum load reaches 375 kN. Obviously, a large load induces significant plastic deformation in the soil.

3.4 Typical bending strain induced in a pile during cyclic loading

Fig. 9 shows variation of bending strain induced in the front pile due to lateral cyclic loading. During the loading process, bending strain induced in the pile increases while it decreases during the unloading process. After each loading-unloading cycle, an incremental bending strain is observed in the front pile. In other words, residual bending strains are induced in the pile after each loading-unloading cycle. This is consistent with the variation of the lateral pile movements with the lateral loading cycles (see Fig. 7). For the residual bending strain induced in the pile, it always increases with the loading cycles. As the cyclic loads increases from 67.5 to 375 kN, the maximum residual bending strain induced in existing piles increases from 50 to 1150 $\mu\epsilon$. If the lateral load is less than 250 kN, the maximum bending strain induced in the existing piles increases with loading cycles. During this cyclic loading period, the maximum bending strain of existing piles increases from 65 to 2050 $\mu\epsilon$. However, a decrease in the maximum bending strain with increasing loading cycles is observed when the lateral load is higher than 250 kN. When the lateral load increases from 250 to 375 kN, the maximum bending strain induced in the pile decreases to be 1530 $\mu\epsilon$. As shown in Fig. 7, residual lateral movement is induced in the pile. In other words, the surrounding soil is displaced away from the pile. Thus, there may be no contact between the upper part of soil and the existing pile. In order to balance the applied horizontal load, the resisting soil mass gradually enlarges to a deep depth. Thus, rotation may occur at the pile toe causing a reduction in the bending strain.

3.5 Relationship between bending strain of piles and cyclic load

Fig. 10(a) shows the relationships between the maximum bending strain of and the cyclic load. Due to constraints of the pile cap and the surrounding soil, the location of the maximum bending strain of piles is below the ground surface. For the front pile (i.e., closer to the loading system), the maximum bending strains are 211, 607, 2186 and 1956 $\mu\epsilon$, respectively, when the applied lateral loads are 62.5, 125, 250 and 375 kN. For the rear pile (i.e., far away from the loading system), induced maximum bending strains are 200, 533, 1400 and 609 $\mu\epsilon$, respectively, when the applied lateral loads are 62.5, 125, 250 and 375 kN. The maximum bending strain induced in the rear pile is much smaller than that in the front pile, especially when the lateral load is large. For the geometry considered in this study, the maximum bending strain induced in the front pile can be up to 3.2 times as large as that in the rear pile.

Fig. 10(b) shows the relationship between the residual bending strain and the cyclic load. The residual bending strain induced in the front pile is also much larger than that in the rear pile. In this test, the maximum residual bending strain induced in the front pile is up to 3.1 times as large as that in the rear pile. For unreinforced concrete, the ultimate tensile strain is 150 $\mu\epsilon$ (American Concrete Institute 2001). Obviously, the maximum and residual bending strain exceeds the tensile strain limit of unreinforced concrete.

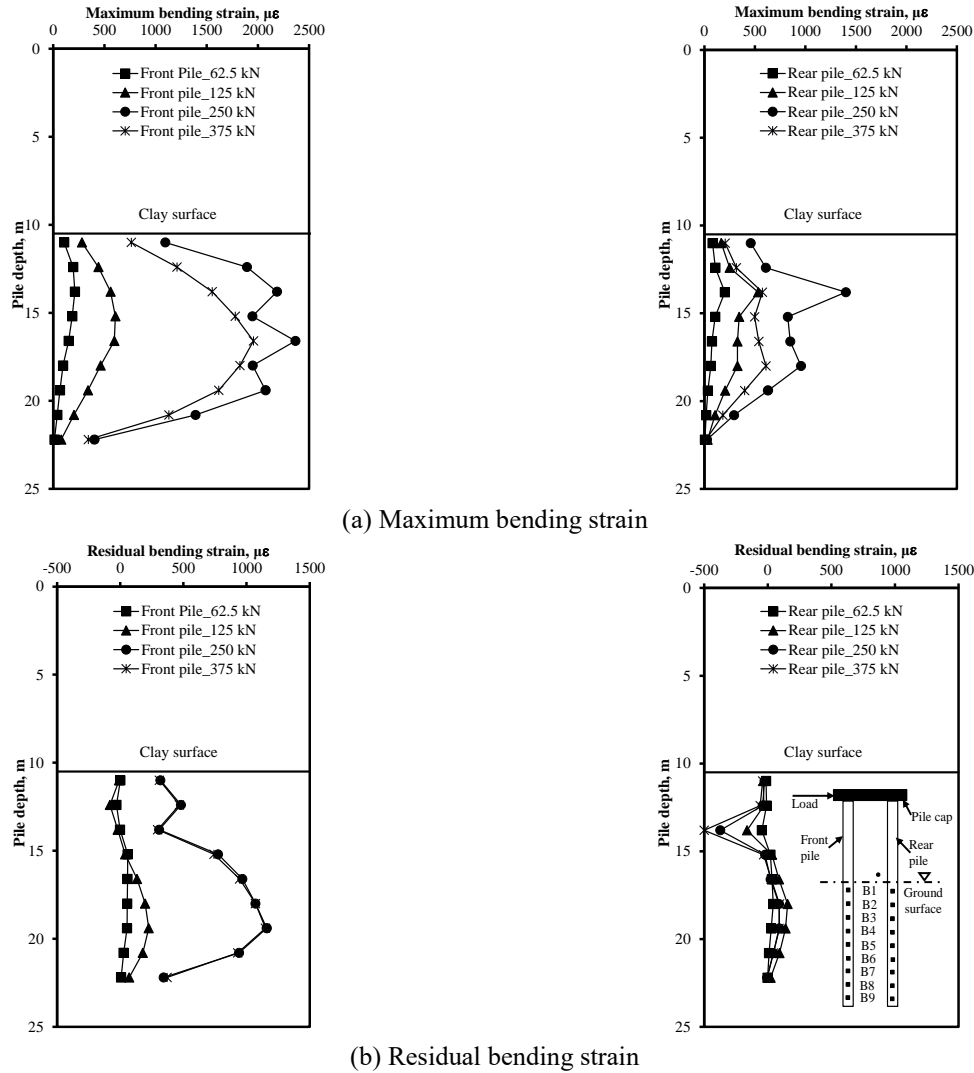


Fig. 10 Relationship between bending strain induced in the piles and applied cyclic load

Thus, much more protection measures should be applied to the front piles to ensure the serviceability and safety of pile foundations in marine deposits. The residual bending strain is much smaller than the maximum bending strain induced in the pile. For the front pile, the ratio of the residual bending strain to the maximum bending strain is in a range of 0.28 to 0.59. Moreover, the ratio of the residual bending strain to the maximum bending strain of the rear pile varies from 0.23 to 0.82.

4. Conclusions

In this study, centrifuge tests were conducted to investigate deformation mechanisms of a pile group due to lateral cyclic loading in kaolin. Based on the measured results, the following conclusions may be drawn:

- As an increase in the applied lateral load, the pile group moves forward, while it moves backward when the load is reduced. After applying each loading-unloading cycle, the pile group cannot move back to its original location. Obviously, cyclic loading induces residual

movement and bending strain in the pile group. This is because plastic deformation is induced in the soil surrounding the piles.

- The maximum and residual lateral movements induced in the pile group increases with the cyclic loads. By increasing the cyclic loads from 62.5 to 375 kN, the maximum and residual pile head movements vary from 26.0 to 1134 mm and from 7.6 to 952 mm, respectively. The ratio of the residual to the maximum pile head movement varies from 0.30 to 0.84 as the cyclic load increases from 62.5 to 375 kN.

- As the applied lateral load increases from 62.5 to 375 kN, the maximum bending strain of the front pile varies from 211 to 2186 $\mu\epsilon$ while the maximum bending strain of rear piles is in a range of 200 to 1400 $\mu\epsilon$. For front and rear piles, ratio of the residual to the maximum bending strain is in a range of 0.23 to 0.82.

- For the geometry considered in this study, the maximum bending strain induced in the front pile is up to 3.2 times as large as that induced in the rear pile. Moreover, the residual bending strain of the front pile is up to 3.1 times as large as that of the rear pile. Thus, much more

protection measures should be applied to front piles to ensure the serviceability and safety of pile foundations.

Acknowledgements

The research described in this paper was financially supported by the Fundamental Research Funds for the Central Universities (2018B56914, 2015B25914, 2018B42414), the National Natural Science Foundation of China (51608170, 51779152 & 51708175), the Natural Science Foundation of Jiangsu Province (BK20160863), the China Postdoctoral Science Foundation (2016M601709 & 2017T100324), the Fundamental Research Funds for the Central Universities (2018B00814) and the Priority Academic Program Development of Jiangsu Higher Education Institutions (PAPD).

References

- Achmus, M., Kuo, Y.S. and Abdel-Rahman, K. (2008), "Behavior of monopile foundations under cyclic lateral load", *Comput. Geotech.*, **36**(5), 725-735.
- Al-Tabbaa, A. (1987), "Permeability and stress-strain response of Speswhite Kaolin", Ph.D. Thesis, University of Cambridge, Cambridge, U.K.
- American Concrete Institute. (2001), *Control of Cracking in Concrete Structures (ACI 224R-01)*, American Concrete Institute, Michigan, U.S.A.
- Asaoka, A. (1978), "Observational procedure of settlement prediction", *Soil. Found.*, **18**(4), 87-101.
- Bolton, M.D. and Stewart, D.I. (1994), "The effect on propped diaphragm walls of rising groundwater in stiff clay", *Géotechnique*, **44**(1), 111-127.
- Brandenberg, S.J., Boulanger, R.W., Kutter, B.L. and Chang, D. (2005), "Behavior of pile foundation in laterally spreading ground during centrifuge tests", *J. Geotech. Geoenviron. Eng.*, **131**(1), 1378-1391.
- Giannakos, S., Gerolymos, N. and Gazetas, G. (2012), "Cyclic lateral response of piles in dry sand: Finite element modeling and validation", *Comput. Geotech.*, **44**, 116-131.
- Gourvenec, S., Acosta-Matinez, H.E. and Randolph, M. F. (2009), "Experimental study of uplift resistance of shallow skirted foundations in clay under transient and sustained concentric loading", *Géotechnique*, **59**(6), 525-537.
- Haldar S. and Babu, G.L.S. (2010), "Failure mechanisms of pile foundations in liquefiable soil: Parametric study", *Int. J. Geomech.*, **10**(2), 74-84.
- Hussien, M.N., Tobita, T., Iai, S. and Karray, M. (2014), "On the influence of vertical loads on the lateral response of pile foundation", *Comput. Geotech.*, **55**, 392-403.
- Jáky, J. (1944), "The coefficient of earth pressure at rest", *J. Soc. Hungarian Arch. Eng.*, **7**, 355-358.
- Kim, Y. and Jeong, S. (2011), "Analysis of soil resistance on laterally loaded piles based on 3D soil-pile interaction", *Comput. Geotech.*, **38**(2), 248-257.
- Kuo, Y.S., Achmus, M. and Abdel-Rahman, K. (2012), "Minimum embedded length of cyclic horizontally loaded monopiles", *J. Geotech. Geoenviron. Eng.*, **138**(3), 357-363.
- Lee, G.T.K. and Ng, C.W.W. (2005), "Effects of advancing open face tunneling on an existing loaded pile", *J. Geotech. Geoenviron. Eng.*, **131**(2), 193-201.
- Lim, S.S. and Liao, J.C. (1999), "Permanent strains of piles in sand due to cyclic lateral loads", *J. Geotech. Geoenviron. Eng.*, **125**(9), 798-802.
- Liu, H.Y., Small, J.C., and Cater, J.P. and Williams, D.J. (2009), "Effects of tunnelling on existing support systems of perpendicularly crossing tunnels", *Comput. Geotech.*, **36**(5), 880-894.
- Long, J.H. and Vanneste, G. (1994), "Effects of cyclic lateral loads on piles in sand", *J. Geotech. Eng.*, **120**(1), 224-244.
- Marshall, A.M. (2009), "Tunnelling in sand its effects on pipelines and piles", Ph.D. Thesis, Cambridge University, Cambridge, U.K.
- Memarpour, M.M., Kimiaei, M., Shayanfar, M. and Khanzadi, M. (2012), "Cyclic lateral response of pile foundations in offshore platforms", *Comput. Geotech.*, **42**, 180-192.
- Ng, C.W.W., Van Laak, P., Tang, W.H., Li, X.S. and Zhang, L.M. (2001), "The Hong Kong geotechnical centrifuge", *Proceedings of the 3rd International Conference on Soft Soil Engineering*, Hong Kong, December.
- Ng, C.W.W., Van Laak, P.A., Zhang, L.M., Tang, W.H., Zong, G.H., Wang, Z.L., Xu, G.M. and Liu, S.H. (2002), "Development of a four-axis robotic manipulator for centrifuge modeling at HKUST", *Proceedings of the International Conference on Physical Modelling in Geotechnics*, St. John's Newfoundland, Canada, July.
- Powrie, W. (1986), "The behaviour of diaphragm walls in clay", Ph.D. Thesis, University of Cambridge, Cambridge, U.K.
- Rahmani, A. and Pak, A. (2012), "Dynamic behavior of pile foundations under cyclic loading in liquefiable soils", *Comput. Geotech.*, **40**, 114-126.
- Randolph, M.F. and Houlsby, G.T. (1984), "The limiting pressure on a circular pile loaded laterally in cohesive soil", *Géotechnique*, **34**(4), 613-623.
- Rollins, K.M., Gerber, T.M., Lane, J.D. and Ashford, S.A. (2005a), "Lateral resistance of a full-scale pile group in liquefied sand", *J. Geotech. Geoenviron. Eng.*, **131**(1), 115-125.
- Rollins, K.M., Lane, J.D. and Gerber, T.M. (2005b), "Measured and computed lateral response of a pile group in sand", *J. Geotech. Geoenviron. Eng.*, **131**(1), 103-114.
- Rollins, K.M., Olsen, R.J., Egbert, J.J., Jensen, D.H., Olsen, K.G. and Garrett, B.H. (2006a), "Pile spacing effects on lateral pile group behaviour: Load tests", *J. Geotech. Geoenviron. Eng.*, **132**(10), 1262-1271.
- Rollins, K.M., Olsen, R.J., Jensen, D.H., Garrett, B.H., Olsen, K.G. and Egbert, J.J. (2006b), "Pile spacing effects on lateral pile group behaviour: Analysis", *J. Geotech. Geoenviron. Eng.*, **132**(10), 1272-1283.
- Rosquoet, F., Thorel, L., Garnier, J. and Canepa, Y. (2007), "Lateral cyclic loading of sand-installed piles", *Soil. Found.*, **47**(5), 821-832.
- Taylor, R.N. (1995), *Geotechnical Centrifuge Technology*, Blackie Academic and Professional, London, U.K.
- Wang, L.Z., Chen, K.X., Hong, Y. and Ng, C.W.W. (2015), "Effect of consolidation on responses of a single pile subjected to lateral soil movements", *Can. Geotech. J.*, **52**(6), 769-782.
- Weaver, T.J., Ashford, S.A. and Rollins, K.M. (2005), "Response of 0.6 m cast-in-steel-shell pile in liquefied soil under lateral loading", *J. Geotech. Geoenviron. Eng.*, **131**(1), 94-102.
- Zhang, C., White, D. and Randolph, M. (2011), "Centrifuge modeling of the cyclic lateral response of a rigid pile in soft clay", *J. Geotech. Geoenviron. Eng.*, **131**(7), 717-729.
- Zhang, Y.T. and Ng, C.W.W. (2017), "Centrifuge modelling of single pile response due to lateral cyclic loading in kaolin clay", *Mar. Georesour. Geotech.*, **35**(7), 999-1007.

